Modifying Dielectrophoretic Response of Nonviable Yeast Cells by Ionic Surfactant Treatment

ARTICLE *in* ANALYTICAL CHEMISTRY · JUNE 2013

Impact Factor: 5.64 · DOI: 10.1021/ac400741v · Source: PubMed

6 AUTHORS, INCLUDING:

Sara Baratchi
RMIT University
36 PUBLICATIONS **616** CITATIONS
SEE PROFILE

Kourosh Kalantar-zadeh
RMIT University
405 PUBLICATIONS **7,642** CITATIONS
SEE PROFILE

Khashayar Khoshmanesh
RMIT University
98 PUBLICATIONS **1,140** CITATIONS
SEE PROFILE

analytical chemistry

Article

pubs.acs.org/ac

Modifying Dielectrophoretic Response of Nonviable Yeast Cells by Ionic Surfactant Treatment

Shi-Yang Tang,*[,†] Wei Zhang,[†] Sara Baratchi,[†,‡] Mahyar Nasabi,[†] Kourosh Kalantar-zadeh,*[,†] and Khashayar Khoshmanesh*[,†]

[†]School of Electrical and Computer Engineering, RMIT University, VIC 3001, Australia

[‡]Health Innovations Research Institute, RMIT University, VIC 3083, Australia

Supporting Information

ABSTRACT: Nonviable cells are essential biosystems, due to the functionalities they offer and their effects on viable cells. Therefore, the separation and immobilization of nonviable cells separately or in the vicinity of viable cells is of great importance for many fundamentals investigations in cell biology. However, most nonviable cells become less polarizable than the surrounding medium at conductivities above 0.01 S/m. This means that in such a medium, dielectrophoresis, despite its great versatilities for manipulation of cells, cannot be employed for immobilizing nonviable cells. Here, we present a novel approach to change the dielectrophoretic (DEP) response of nonviable yeast cells by treating them with low concentrations of ionic surfactants such as sodium dodecyl sulfate. After this treatment, they exhibit a strong positive DEP response, even at high medium conductivities. The capability of this treatment is demonstrated in two proof-of-concept experiments. First, we show the sorting and immobilization of viable and nonviable yeast cells, along consecutive microelectrode arrays. Second, we demonstrate the immobilization of viable and nonviable cells in the vicinity of each other along the same microelectrode array. The proposed technique allows DEP platforms to be utilized for the immobilization and subsequent postanalysis of both viable and nonviable cells with and without the presence of each other.

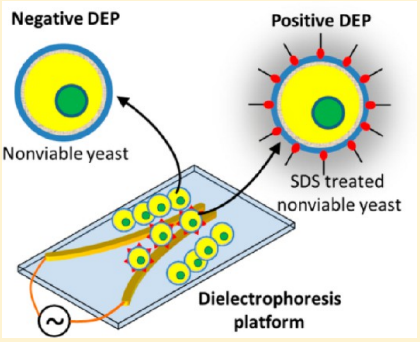

Dielectrophoresis, the induced motion of neutral particles in nonuniform electric fields, offers a great potential for the manipulation of micro/nano particles in microfluidics.[1−3] A variety of investigations has been dedicated to innovative applications of dielectrophoresis in biomedical and biotechnology fields. Different bioparticles have been investigated using dielectrophoretic (DEP)-based microfluidic platforms, including: cell organelles such as DNA,[4] proteins,[5] chromosome,[6] and mitochondria;[7] mammalian cells such as blood cells,[8] stem cells[9] and neurons;[10] model cells such as yeast;[11,12] and multicellular organisms.[13] In particular, analysis of cells using dielectrophoresis is still a hot research topic due to the importance of cells in the diagnosis and prognosis of diseases, drug discoveries, and understanding the fundamentals of their functionalities. Dielectrophoresis enables the rapid and efficient sorting of cells based on their cytoplasmic properties,[11,14,15] dimensions[16,17] or membrane surface properties,[18,19] immobilization of viable cells between the microelectrodes for further characterization against different drugs,[20−23] and also interfacing with different technologies such as environmental scanning electron microscopy.[24]

The DEP response of cells depends on the dielectric properties of both the cells and surrounding medium. If the cell is more polarizable than the medium, it will experience a positive DEP force and be pushed toward the microelectrodes. Conversely, if the cell is less polarizable than the suspending medium, it will experience a negative DEP force and be repelled from the microelectrodes.[1] In many applications, DEP systems are utilized for the immobilization of viable cells. As such, the cells hold still to avoid any localized movements. Such immobilization processes are important for the investigation of cell properties via spectroscopic and optical systems, for which a certain data acquisition time is required.[20]

Yeast cells have been widely used as a model organism for studying fundamental cellular processes and different diseases such as cancer and neurodegenerative disorders.[25] While, there are many reports on the DEP manipulations of viable yeast cells, rarely any reports on the immobilization of nonviable cells can be found. Although nonviable cells are not able to proliferate, they remain as important biosystems for studying many fundamental properties of cells. They still perform many functions, even after losing their viability. Such functionalities allow nonviable cells to send signals/chemicals to the surrounding medium that can influence the metabolism and viability of surrounding cells. For example, Herker et al.[26] found that the death of aging yeast cells can improve the survival of surrounding cells due to the releasing of cytoplasmic substances. Similarly, Váchová et al.[27] discovered that the ammonia signals released from aging yeast colonies can trigger metabolic changes within the surrounding cells and improve

Received: March 11, 2013
Accepted: June 1, 2013
Published: June 1, 2013

   dx.doi.org/10.1021/ac400741v | *Anal. Chem.* 2013, 85, 6364−6371

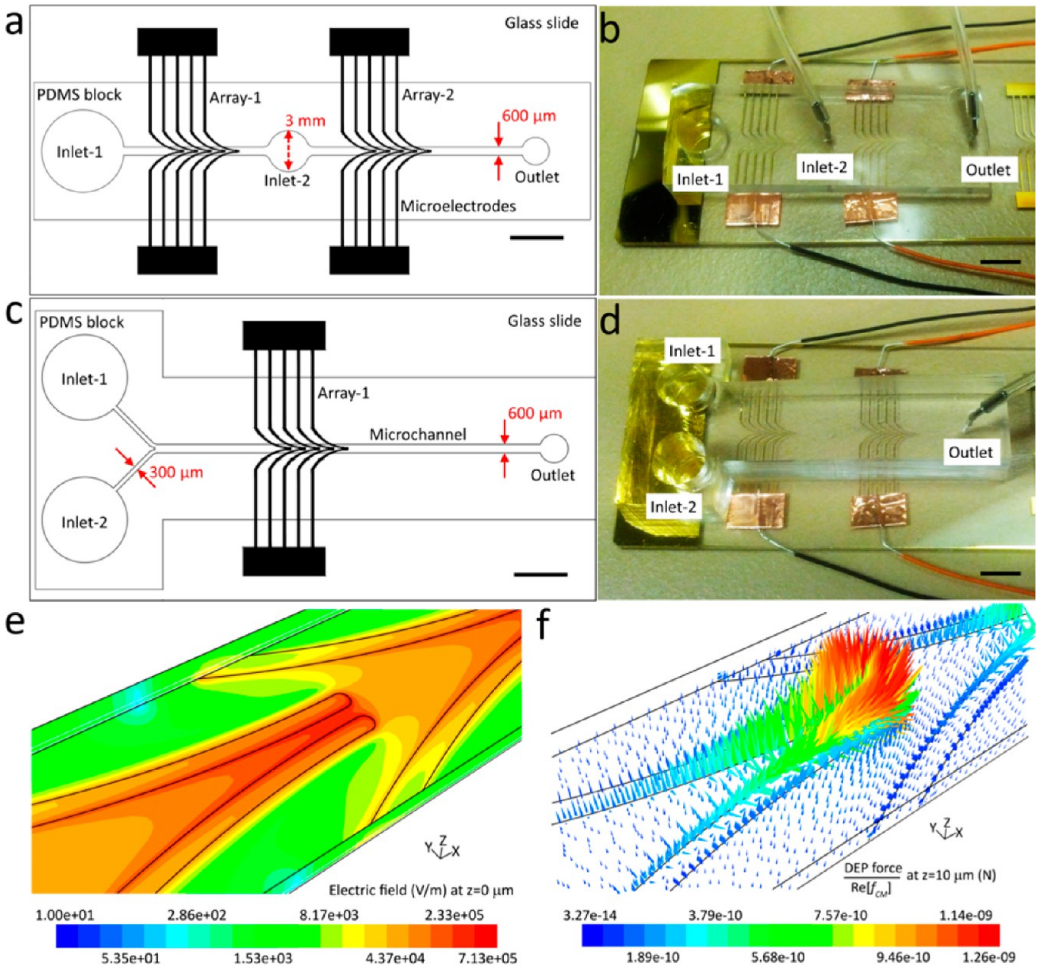

Figure 1. Specifications of the applied DEP systems: (a–b) for the first set of experiments, a PDMS microchannel with two cascaded inlets was assembled onto a DEP platform equipped with two microelectrode arrays, and (c–d) for the second set of experiments, a PDMS microchannel with two parallel inlets was assembled onto a DEP platform. The wires were bonded to the microelectrode pads by copper tapes. Scale bars are 5 mm. Contours of electric field and DEP force/$Re[f_{CM}]$ at the levitation height of z = 10 μm are shown in (e) and (f), respectively, produced by curved microelectrodes at 30 V_{p-p}, obtained by numerical simulations.

their survival. This concept can be further extended by investigating the effect of drug treated nonviable cells on surrounding viable cells. The immobilization of nonviable yeast cells can also be critical in understanding the migration of immune cells toward the inflammation sites that are caused by the accumulation of damaged or dead yeast cells.[28] Furthermore, it enables the investigation of the phagocytosis mechanism in response to dead pathogenic yeast species, such as *Candida albicans* and *Candida dubliniensis*.[29,30] Moreover, immobilization of nonviable yeasts enables creating model cell clusters composed of both viable and nonviable cells to mimic the performance of dysfunctional tissues.

Using dielectrophoresis for immobilization of nonviable cells is rather challenging. In doing so, the electrical conductivity of the medium should be reduced to very low levels to ensure the nonviable cells remain more polarized than the surrounding medium.[31] For example, Talary et al.[32] has demonstrated the trapping of nonviable yeast cells at a medium conductivity of 0.0078 S/m and applying frequencies lower than ~500 kHz. Our calculations indicate that the positive DEP response of nonviable yeast cells vanishes at medium conductivities higher than ~0.01 S/m (Figure S1 of the Supporting Information). However, buffers with such low conductivities are not suitable for many biological experiments, as they cannot sustain the integrity of viable cells due to lack of ion components such as calcium, sodium, and potassium in the buffer and can lead to an excessive efflux of cytoplasmic ions into the buffer.[33] An alternative solution to immobilize the nonviable cells is to push them toward the regions of low electric field gradient under negative DEP forces and trap them at those regions. Although this method does not need the decrease in medium conductivity, it requires the implementation of mechanical barriers such as cylindrical posts within the channel to shelter the trapped cells against the hydrodynamic drag force.[15,34]

Several DEP-based methods have been proposed to enable the immobilization of low polarizable particles. For example, Khoshmanesh et al.[35,36] demonstrated the trapping of polystyrene microparticles by utilizing highly conductive carbon nanotubes (CNTs). The patterned CNTs between the microelectrodes served as nanoelectrodes, producing a strong electric field at their free ends. Additionally, the overall conductivity of polystyrene particles increased due to the CNT coating, enabling their immobilization. A similar concept was utilized by Zhou et al.[37] to capture and detect low numbers of *Escherichia. coli* bacteria. Disadvantageously, in both aforementioned works, the patterned CNTs between microelectrodes distorted the original electric field and eventually led to electrical short circuits. More importantly, the possible

dx.doi.org/10.1021/ac400741v | *Anal. Chem.* 2013, 85, 6364–6371

biocompatibility and cytotoxicity of CNTs can be another concern.[38] Other nanoparticles with high polarizability, such as gold or silver nanoparticles, can also be utilized as an alternative to CNTs.[39,40] However, similar issues such as electrical short circuits, caused by the aggregation of nanoparticles between microelectrodes, may also occur.

Modification of the surface properties of cells is the key factors in tuning their DEP response to achieve desired cell manipulations. Low concentration (<1%) nonionic surfactant solutions are routinely used in microfluidic experiments to avoid cell agglomeration without disrupting the integrity of a viable cell's plasma membrane.[11,12,41] However, there is no report on implementing surfactants to modify the DEP response of nonviable cells with their low polarizability.

In this work, we present a novel approach to modify the DEP response of nonviable (methanol treated) yeast cells by treating them with a low concentration of ionic surfactants, such as sodium dodecyl sulfate (SDS). This enables us to immobilize the nonviable cells at highly conductive media (σ_{medium} > 0.05 S/m), which is on the order of commonly used biological buffers. Upon SDS treatment, the overall conductivity of nonviable cells is increased, making them exhibit a positive DEP response. The crossover frequency of SDS-treated nonviable cells is measured at different medium conductivities to estimate the induced surface conductivity. Two experiments are conducted in order to demonstrate the potential applications of the SDS modification. First, we demonstrate the sorting and immobilization of viable and nonviable cells along two consecutive microelectrode arrays by using a microchannel with two cascaded inlets. Second, we exhibit the immobilization of viable and nonviable cells, next to each other, along the same microelectrode pair by using a microchannel with two parallel inlets.

2. MATERIALS AND METHODS

DEP Chip Design and Fabrication. The DEP system takes advantage of curved microelectrodes, as detailed in ref 11. The width of microelectrodes is 50 μm, the gap between the tips of the microelectrodes is 40 μm, and the spacing between the sequential microelectrode pairs is 1000 μm. A microchannel with two cascaded or parallel inlet reservoirs was assembled onto the glass substrate (Figure 1), which accommodates the microelectrodes to form the DEP systems. Both microchannels have a width of 600 μm and a height of 75 μm. The plan views of the DEP systems are shown in Figure 1, panels a and c.

Microelectrode arrays were made of thin layers of chromium/gold (100 nm/100 nm) and patterned onto microscopic glass slides (1 × 3 in.), using the standard photolithography technique.[42] The polydimethylsiloxane (PDMS) microchannels were also fabricated using standard photolithography techniques.[42] The PDMS microchannel was located on the patterned glass slide (Figure 1, panels b and d). The integrated system was then clamped between two 3 mm thick polymethyl methacrylate (PMMA) sheets to avoid any leakage (see Figure S2 of the Supporting Information S2).

Strong nonuniform electric fields can be produced with the curved microelectrodes within the microchannel.[11,12] In order to calculate the distribution of electric field and DEP forces produced by the curved microelectrodes, we developed a numerical model, using ANSYS Fluent 6.3 (Canonsburg, PA, USA), as detailed in Figure S3 of the Supporting Information. The numerical simulation shown in Figure 1e indicates that the electric field smoothly increases along the microelectrode structure, reaching a peak of 7.13 × 10^5 V/m at the tips. This enables cells to form pearl chains at the entrance of microelectrodes and thus improves the trapping efficiency of the system.[12,35] The distribution of DEP forces produced by curved microelectrodes is shown in Figure 1f. The DEP force is calculated by considering the diameter of cells as 7 μm, which corresponds to nonviable yeasts, as detailed in Figure S4 of the Supporting Information. The simulations predict that the magnitude of DEP force/$Re[f_{CM}]$ reaches a maximum of 1.26 nN at the tip region at the levitation height of z = 10 μm. The values of the medium conductivity and the applied frequency can be changed to vary $Re[f_{CM}]$ and consequently to obtain the desired DEP forces.

Preparation of Yeast Cell Suspension. *Saccharomyces cerevisiae* yeast cells (powder, Sigma-Aldrich) were chosen as the target cells. For preparation of viable cell suspension, 2 mg of cell powder was mixed with 8 mL of low electrical conductivity buffer (LEC, 8.5% w/v sucrose and 0.3% w/v dextrose) to yield a cell concentration of 0.25 mg/mL (~1.5 × 10^5 cells/mL). The cells were further kept in an ultrasonic water bath at 37 °C for 30 min to prevent the agglomeration of cells. For the preparation of nonviable cell suspension, 2 mg of yeast powder was dissolved in 8 mL of a 50−50% DI water−methanol solution and kept in a water bath at 37 °C for 30 min to yield a cell concentration of 0.25 mg/mL. The sample was then centrifuged at 1500 rpm for 5 min, and the cells were washed with LEC buffer to remove the excess methanol. For the preparation of viable−nonviable cell suspensions, mixtures of 25−75%, 50−50%, and 75−25% viable−nonviable cell suspensions with a total cell concentration of 0.25 mg/mL were prepared. The microchannel was washed with a 2% bovine serum albumin (BSA) suspension before each experiment with a flow rate of 10 μL/min for 30 min to prevent the adhesion of cells to the glass substrate and channel walls. The electrical conductivity of the buffer was adjusted by adding appropriate amounts of phosphate-buffered saline (PBS) into the cell suspension.

Surfactant Treatment and Labeling with Fluorescent Probes. SDS was used for treating the nonviable cells. SDS is an ionic surfactant, which consists of two major components, a hydrophilic headgroup and a hydrophobic tail group (Figure 2a). In our designed protocol, 10 mg of SDS powder was dissolved into 5 mL of LEC buffer to obtain a 2 mg/mL SDS/LEC buffer. Next, 50 μL of 1 mg/mL propidium idodie (PI) was added into the SDS/LEC buffer to yield a PI concentration of 10 μg/mL. The procedure of nonviable cells treatment is schematically shown in Figure 2b. Given that the cell wall of yeast contains β-glucan (60%), chitin (1−3%), and mannoproteins (40%),[43] the SDS molecules are able to noncovalently bind to the mannoproteins.[44] With dependence on the number of bounded SDS molecules, the surface conductivity of nonviable yeasts can be significantly enhanced. Moreover, if SDS molecules can penetrate into the cell wall, their hydrophobic tail (as shown in Figure 2b) might be able to bind to the hydrophobic tail of the phospholipid molecules that exist within the lipid bilayer of the plasma membrane.[33] The immobilization and staining of nonviable cells were conducted in the presence of the SDS/LEC buffer.

Cell Surface Coating Characterization. Raman measurements were performed using an In-Via Raman microscope (Renishaw Plc.). A 13 mW, 514 nm laser was used as the excitation source. A 50× objective lens was utilized to focus the excitation laser beam and to collect the Raman spectra in back-

dx.doi.org/10.1021/ac400741v | Anal. Chem. 2013, 85, 6364−6371

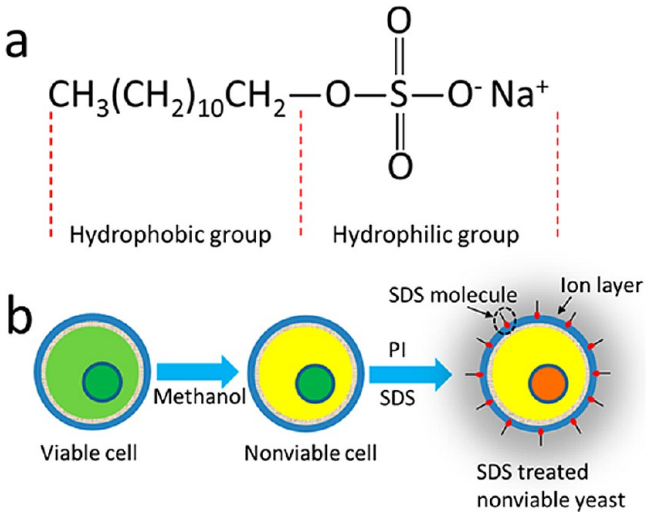

Figure 2. (a) The chemical structure of SDS and (b) the process obtaining SDS-treated nonviable cells.

reflection with an acquisition time of 10 s. For the case of SDS-treated nonviable cells, the cells were centrifuged at 1500 rpm for 5 min to remove the excess SDS.

Experimental Setup. Syringe pumps (Harvard Apparatus, PHD 2000) were employed to extract the cell suspension from or infused into the outlet/inlet ports at desired flow rates. An inverted optical microscope (Nikon Eclipse, TE 2000) was used in order to obverse the response of cells within the microfluidic system. Objective lenses (4× , 10×) with appropriate fluorescence filters of 525/595 nm were used for obtaining multicolor images in the presence of PI. A signal generator (Tabor, 2572A 100 MHz dual-channel) was applied to energize the microelectrodes with a sine wave of viable frequencies, ranging from 25 kHz to 40 MHz. A high precision conductivity meter (ECTestr11+, Eutech Instruments) was utilized to measure the conductivity of suspensions.

3. THEORY

With the assumption that yeast cells have spherical structures, they experience a time-averaged DEP force as given below:[1]

$$\bar{F}_{DEP} = 2\pi r^3 \varepsilon_{medium} Re[f_{CM}] \nabla E_{rms}^2 \quad (1)$$

where r is the radius of cells, ε_{medium} is the permittivity of the suspending medium, E_{rms} is the root-mean-square of the applied electric field, and f_{CM} is the Clausius−Mossotti factor of the cells, describing their polarization with respect to the surrounding medium, which is calculated as[1]

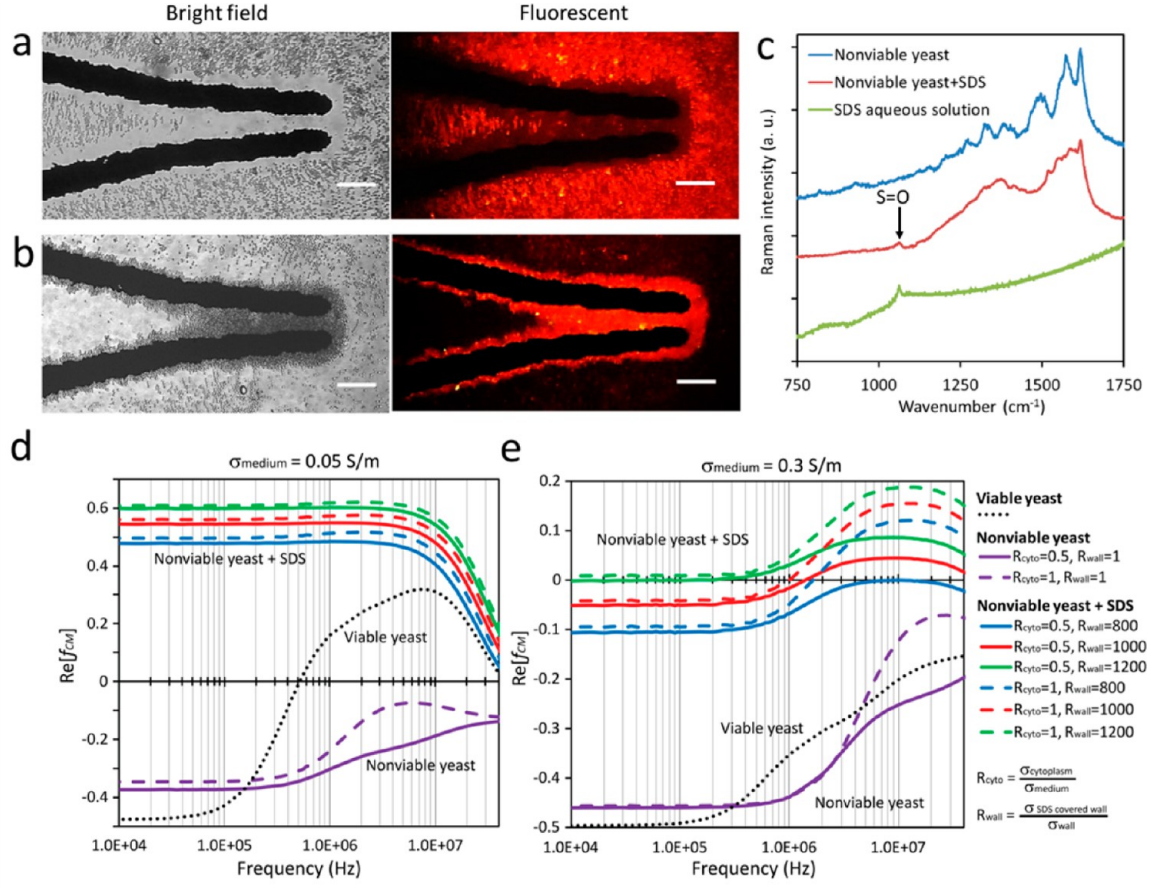

Figure 3. Characterization of SDS-treated nonviable cells: (panels a−b) the DEP response of nonviable yeast labeled with PI with and without SDS treatment obtained by the open-top DEP system. The electrical conductivity of the medium was set to 0.1 S/m, while the magnitude and frequency of the AC signal were set to 30 $V_{p\text{-}p}$ and 10 MHz. Scale bars are 100 μm. (c) Examples of Raman spectra of single nonviable cell and SDS-treated nonviable cell in the 750−1750 cm^{-1} region (SDS aqueous solution Raman spectrum is included as a reference), and the $Re[f_{CM}]$ spectra of nonviable yeast cells treated by 0.2% SDS, nonviable yeast, and viable yeast obtained by the spherical multishell model at the medium conductivity of (d) 0.05 and (e) 0.3 S/m.

dx.doi.org/10.1021/ac400741v | Anal. Chem. 2013, 85, 6364−6371

$$f_{CM} = \frac{\varepsilon^*_{cell} - \varepsilon^*_{medium}}{\varepsilon^*_{cell} + 2\varepsilon^*_{medium}} \quad (2)$$

$$\varepsilon^* = \varepsilon - \frac{i\sigma}{2\pi f}, \quad i = \sqrt{-1} \quad (3)$$

where ε^* is the complex permittivity, ε is the permittivity, σ is the electrical conductivity, and f is the frequency of the applied AC signal. With consideration that yeast cells have a complex structure consisting of cytoplasm, plasma membrane, and an outer wall surrounding the cell,[45] their $Re[f_{CM}]$ is calculated using the spherical multishell model, as given in Figure S4 of the Supporting Information. The geometrical and electrical properties of the viable cells are based on the values given by Huang et al.,[45] as presented in Figure S4 of the Supporting Information.

Alternatively, for the nonviable cells, while their geometrical properties were adopted from Huang et al.,[45] their electrical properties were altered to take into account the impact of different medium conductivities, as well as the SDS treatment. With consideration that the integrity of nonviable cells' plasma membranes are compromised, we assumed that the conductivity of the cytoplasm is proportional to that of the surrounding medium, as given in eq 4. A similar concept has been used by Gascoyne et al.[46] to estimate the cytoplasm conductivity of malaria-infected erythrocytes. With consideration that the conductivity of cell surface is significantly enhanced due to accumulation of the SDS molecules (Figure2, panel b), we assumed that the conductivity of the outer wall is proportional to the concentration of SDS within the buffer, as given in eq 5. A similar concept has been used by Cui et al.[47] to consider the surface charges induced on the surface of polystyrene particles when exposed to ionic electrolytes.

$$\sigma_{cyto} \propto \sigma_{medium} \quad (4)$$

$$\sigma_{wall} \propto \text{SDS concentration} \quad (5)$$

In doing so, we defined R_{cyto} as $\sigma_{cyto}/\sigma_{medium}$ and R_{wall} as $\sigma_{SDS\ covered\ wall}/\sigma_{wall}$ and varied these ratios in order to obtain the $Re[f_{CM}]$ of SDS-treated nonviable cells, as discussed in Figure 3.

4. RESULTS AND DISCUSSION

In order to characterize the DEP response of SDS-treated nonviable cells, we carried out a set of experiments by applying cells into an open-top chamber that was placed onto the microelectrodes. The chamber was created by punching a circular hole with a diameter of 6 mm and a height of 5 mm within a PDMS block (see Figure S5 of the Supporting Information). This simple configuration enabled us to conduct quick DEP experiments with no liquid flow.

In so doing, 100 μL of nonviable cell suspension stained with PI was applied into the PDMS chamber. The electric conductivity of the buffer was set to 0.1 S/m, while the voltage and frequency of the applied AC signal were set to 30 $V_{p\text{-}p}$ and 10 MHz, respectively. Under these conditions, the nonviable cells experienced a strong negative DEP response and were repelled from the microelectrodes, as demonstrated in Figure 3a. However, the addition of 2 mg/mL SDS to the suspension of nonviable cells changed their DEP response, as all cells experienced a strong positive DEP response and were immobilized between the microelectrodes, as seen in Figure 3b.

The conductivity measured for the SDS/LEC buffer with the SDS concentration of 2 mg/mL was 0.028 S/m, which is much lower than the cytoplasm conductivity of viable yeast cells.[45] Therefore, the change of the nonviable cell's DEP response is not due to the increase of their cytoplasm conductivity.

We hypothesize that the significant change of DEP response observed for SDS-treated nonviable cells is attributed to the coating of SDS molecules on the cell surface. A series of Raman measurements (Figure 3c) were conducted to examine the existence of the SDS coating on the cell surface. All measurements were carried out on a quartz substrate covered with a thin layer of chromium/gold to avoid any interfering background signal. First, we conducted measurements on an SDS aqueous solution (2 mg/mL) and observed the S═O stretching vibration band at the peak shift of 1061 cm^{-1}.[48] Next, we examined the Raman signature of nonviable cells; several peak shifts in the region of 1250 to 1750 cm^{-1} were observed, which can be attributed to the organic chemical bonds, including C−H deformation band, C═N, C═O, C−N, and C═C stretching vibrations.[49−51] No peak shift was observed for S═O at 1061 cm^{-1}. However, after treating the nonviable cells with SDS, apart from the repeatable chemical bonds in the region of 1250 to 1750 cm^{-1}, a new peak shift emerged at 1061 cm^{-1}, confirming the attachment of SDS on the cell surface.

In order to estimate the SDS-induced surface conductivity, we measured the crossover frequency of nonviable cells at different medium conductivities using the open-top DEP system. For nonviable cells (without SDS treatment), a negative DEP response was observed for all medium conductivities ranging from 0.05 to 0.335 S/m across the entire frequencies range from 25 kHz to 40 MHz. Lower frequencies were not tried in order to avoid any electrochemical reactions at the surface of microelectrodes and also unwanted electrothermal vortices at the tip region. Alternatively, when the concentration of SDS was set to 2 mg/mL, the nonviable cells experienced a positive DEP response at medium conductivities of 0.05, 0.1, and 0.18 S/m across the entire frequencies ranging from 25 kHz to 40 MHz. By increasing the medium conductivity to 0.3 S/m, the cells exhibited a positive DEP response at frequencies higher than 300 kHz before which the DEP response of the cells was so weak that almost no motion could be observed. However, further increase of medium conductivity to 0.335 S/m led to a crossover frequency of 700 ± 100 kHz, after which the cells exhibited a positive DEP response. Using the aforementioned crossover frequencies, the $Re[f_{CM}]$ of SDS-treated nonviable cells was calculated, using the spherical multishell model and by varying the ratios of R_{cyto} and R_{wall} between 0.5 and 1 and 800−1200, respectively. The calculated $Re[f_{CM}]$ curves for the medium conductivities of 0.05 and 0.3 S/m are given in Figure 3, panels d−e, while the $Re[f_{CM}]$ curves corresponding to other medium conductivities are given in Figure S6 of the Supporting Information. Figure 3d suggests that $R_{wall} \geq 800$ guarantees the positive DEP response of cells at 40 MHz at the medium conductivity of 0.05 S/m, as observed in our measurements. Alternatively, Figure 3e indicates that $R_{wall} \geq 1200$ assures the positive DEP response of cells at frequencies higher than 300 kHz at the medium conductivity of 0.3 S/m, as observed in our measurements.

It should be noted that the application of other ionic surfactants such as cetrimonium bromide (CTAB) and sodium dodecyl benzene sulfonate (SDBS) to nonviable cells resulted in the positive DEP response of cells at medium electrical conductivities as high as 0.1 S/m (given in Figure S7 of the

dx.doi.org/10.1021/ac400741v | Anal. Chem. 2013, 85, 6364−6371

Supporting Information), similar to that observed for SDS. In contrast, the application of nonionic surfactants such as X-305 and X-100 did not significantly change the DEP response of nonviable cells, and the cells exhibited a negative DEP response at the medium electrical conductivities higher than 0.005 S/m.

We demonstrated that we can immobilize nonviable cells at relatively highly conductive media (σ_{medium} = 0.335 S/m) that has not been shown previously.[11,12,31,32] The Raman experiments proved the coating of SDS molecules on the cell surface and the DEP experiments suggested that the SDS coating has increased the polarizability of the nonviable cells.

The benefits of immobilizing nonviable cells are demonstrated in two proof-of-concept experiments. In the first set of experiments, a PDMS channel with two cascaded inlets was used as shown in Figure 1 (panels a and b). A cell suspension with a viable−nonviable cell ratio of 25% to 75% was applied to Inlet-1 (Figure 4a). The electrical conductivity of the medium at the reservoir was set to 0.05 S/m to guarantee that viable cells can be efficiently immobilized; however, higher medium conductivities can be used (>0.3 S/m) if only the immobilization of nonviable cells is required. A flow rate of 2 μL/min was maintained at the outlet. The magnitude and frequency of the AC signal applied to the first microelectrode array were set to 30 V_{p-p} and 7 MHz, respectively. This frequency was chosen as the viable cells experience the maximum positive DEP force, and at the same time the difference between the DEP forces experienced by viable and nonviable cells was maximum, according to the $Re[f_{CM}]$ spectra for viable and nonviable cells given in Figure 3d.

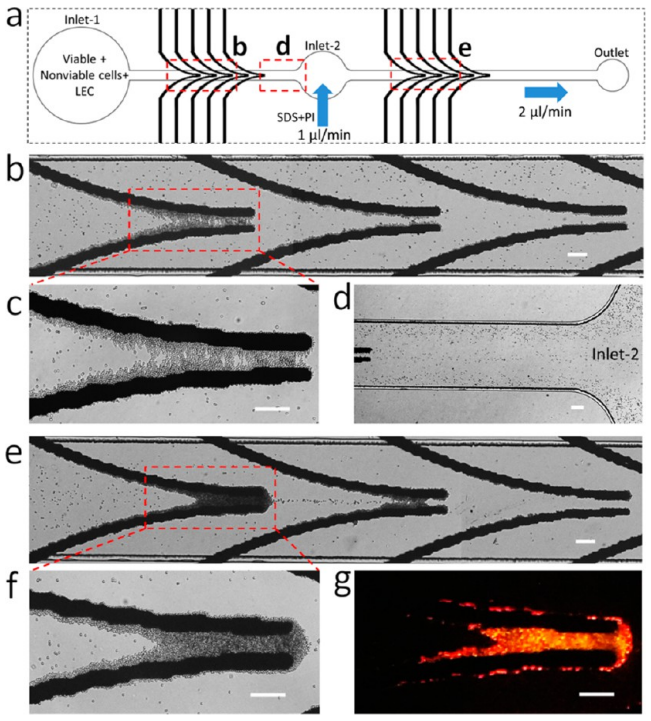

Figure 4. Immobilizing viable and nonviable cells in cascaded microelectrode arrays: (a) schematics of the DEP system (b) shows the sorting of viable and nonviable yeast cells on the first microelectrode array, when the flow rate and electrical conductivity of the medium were set to 2 μL/min and 0.05 S/m, while the magnitude and frequency of the AC signal were set to 30 V_{p-p} and 7 MHz. (c) Magnified image of immobilized viable cells over the first microelectrode pair of the first array (d) shows the entrance to Inlet-2 and (e) shows the immobilization of nonviable cells on the second microelectrode array after treatment with SDS and labeled with PI via Inlet-2. (f) Magnified image of immobilized nonviable cells over the first microelectrode pair of the second array, when the electrical conductivity of the medium reached 0.054 S/m, while the magnitude and frequency of the AC signal were set to 30 V_{p-p} and 7 MHz and (g) shows the fluorescent image of nonviable cells stained with PI. Images were taken 6 min after the application of the electric field to the second microelectrode array. Scale bars are 100 μm.

Figure 4b shows that under this arrangement, most of the viable cells were immobilized over the first microelectrode pair, while a few of them were immobilized over the next two microelectrode pairs. Figure 4c shows the magnified image of viable cells immobilized over the first microelectrode pair just 6 min after the application of cells into the system. Alternatively, most of the nonviable cells were deflected toward the channel sidewalls. A small portion of nonviable cells, which were moving close to the microelectrode tips were pushed to upper levitation heights and passed through the first microelectrode array. Figure 3d shows the repelled nonviable cells before entering the Inlet-2.

The second syringe pump was utilized (see Figure 1b) to inject the SDS/LEC/PI buffer with a SDS concentration of 4 mg/mL and a PI concentration of 20 μg/mL at a flow rate of 1 μL/min into Inlet-2. The dimensions of Inlet-2 were chosen to enable the efficient mixing of SDS/LEC/PI buffer with the nonviable cell suspension under the applied flow rates (see Figure S8 of the Supporting Information). The concentration of the SDS and PI stain was halved after mixing with the nonviable cell suspension coming from Inlet-1. This increased the medium conductivity of the buffer to 0.054 S/m before reaching the second microelectrode array.

The magnitude and frequency of the AC signal applied to the second microelectrode array were set to 30 V_{p-p} and 7 MHz, respectively, to induce a strong positive DEP force on SDS-treated nonviable cells, as shown in Figure 3d. Under this arrangement, most of the nonviable cells were immobilized at the first two microelectrode pairs of the second array, as shown in Figure 4e. Elongating the duration of experiment increased the density of immobilized cells and led to formation of a multilayer of cells at the tip region. The cells at the upper layers experienced a smaller DEP force but a stronger drag force. Therefore after a certain duration, the microelectrodes became saturated and the trapped cells start to detach (see Figure S9 of the Supporting Information). Figure 4f shows the magnified image of the first pair of microelectrodes 6 min after the application of cells. The application of PI into the Inlet-2 enabled the staining of nonviable cells, as shown in Figure 4g. The performance of the system was further examined with different viable−nonviable cell ratios of 50−50% and 75−25%, as shown in Figure S10 of the Supporting Information. Increasing the ratio of viable−nonviable cells led to the accumulation of more viable cells on the first microelectrode array, while less nonviable cells were immobilized on the second microelectrode array.

This set of experiments demonstrated that the nonviable cells could immediately be immobilized after the SDS treatment. This enables the sorting and consequent immobilization of both viable and nonviable cells at predetermined locations of the microfluidic system. Such a platform can be used for analyzing chemicals released from both the viable and nonviable cells and also to investigate the response of them to different physical and chemical stimuli using conventional buffers with large ionic conductivities.

dx.doi.org/10.1021/ac400741v | Anal. Chem. 2013, 85, 6364−6371

In the second set of experiments, a microchannel with two parallel inlets was placed on the same microelectrode array, as shown in Figure 1, panels c and d, in order to immobilize both viable and nonviable cells on the same pair of microelectrodes. In so doing, 100 μL of viable cell suspension was added into the Inlet-1, while 100 μL of PI-stained nonviable cells treated with the SDS/LEC buffer at a SDS concentration of 2 mg/mL was added into the Inlet-2 (Figure 5a). The electrical conductivity

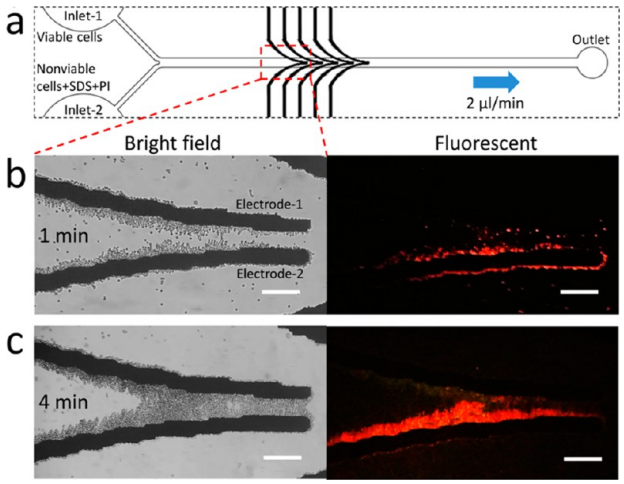

Figure 5. Immobilization of viable and nonviable cells in the same microelectrode pair: (a) schematics of the DEP system. Immobilization of both viable and PI-labeled nonviable cells side by side in the same pair of microelectrodes using the microchannel with two parallel inlets, (b) 1 min and (c) 4 min after the application of electric field. The flow rate and electrical conductivity of the medium were set to 2 μL/min and 0.05 S/m, while the magnitude and frequency of the applied AC signal were set to 30 $V_{p\text{-}p}$ and 7 MHz, respectively. Scale bars are 100 μm.

of the media at both reservoirs was set to 0.05 S/m, while the flow rate along the main channel was set to 2 μL/min. The magnitude and frequency of the applied AC signal were set to 30 $V_{p\text{-}p}$ and 7 MHz, respectively. Both the viable and SDS-treated nonviable cells experienced the maximum positive DEP force under the chosen medium conductivity and the applied AC signal frequency (see Figure 3d). The level of liquid within the two inlets was carefully adjusted to keep a balance between the incoming flows. The flow was purely laminar, due to very low Reynolds number (Re < 0.1), and the mixing of incoming flows only happened at the interface, as evidenced by the formation of a clear boundary between the viable and nonviable cell suspensions along the middle of the microchannel (see Figure S11 of the Supporting Information). Long chains of viable and nonviable stained cells were immobilized along electrode-1 and electrode-2, as shown in Figure 5b. The chains elongated gradually until bridging the opposite microelectrodes after 3 min. Continuing the process led to immobilization of cells on top of each other to form multilayer chains of cells. Even in this case, a clear boundary was observed between the immobilized viable and nonviable cells (Figure 5c). The inlet cell suspensions were replaced with a cell-free buffer after the desired densities of cells were immobilized between the microelectrodes.

This second set of experiments showed the possibility of placing viable and nonviable cells in the vicinity of one another. Such an arrangement allows for the analysis of viable cell responses in the presence of nonviable cell clusters, using relatively highly conductive buffer media to maintain the viability of viable cells.

5. CONCLUSION

We demonstrated that the DEP response of nonviable cells can be altered by treating them with ionic surfactants, such as SDS. The SDS molecules coat the exterior wall of nonviable cells, as confirmed by Raman spectroscopy. We used a DEP system empowered with curved microelectrodes to manipulate SDS-treated nonviable yeast cells within a microfluidic system. The outcomes are summarized as follows: (1) The SDS treatment increased the surface conductivity of nonviable cells, allowing them to experience a strong positive DEP force and, consequently, be immobilized along the microelectrodes, even at high medium electrical conductivities of 0.335 S/m. (2) By employing a microchannel with two cascaded inlets, we demonstrated the sorting of viable and nonviable cells, immobilized the viable cells along the first microelectrode array, and immobilized the nonviable cells along the second microelectrode array, following SDS treatment via the second inlet. (3) Using a microchannel with two parallel inlets, we showed the possibility of immobilizing both viable and nonviable cells in the vicinity of each other with minimum lateral mixing.

This novel surface treatment can readily be adopted by other DEP systems to achieve the capability of manipulating nonviable yeast cells. The work can be further extended by the following: (1) interfacing immobilized nonviable yeast cells with different off-chip technologies, such as confocal Raman and florescence microscopy. (2) Assembling customized clusters of viable and nonviable yeast cells in intimate contact with each other for investigating fundamentals, such as studying the signaling/exchanges of chemical components between the two clusters and understanding the effects of nonviable cells on viable cells in a microfluidic environment.

■ ASSOCIATED CONTENT

Ⓢ Supporting Information

Additional information as noted in text. This material is available free of charge via the Internet at http://pubs.acs.org.

■ AUTHOR INFORMATION

Corresponding Author

*K.Khoshmanesh: e-mail, khashayar.khoshmanesh@rmit.edu.au. K. Kalantarzadeh: e-mail, kourosh.kalantar@rmit.edu.au. S.T.: e-mail, shiyang.tang@rmit.edu.au. Tel: +61 (03) 99252851.

Notes

The authors declare no competing financial interest.

■ ACKNOWLEDGMENTS

K. Khoshmanesh acknowledges the Australian Research Council for funding under Discovery Early Career Researcher Award (DECRA) scheme (Grant DE120101402).

■ REFERENCES

(1) Morgan, H.; Green, N. G. *AC Electrokinetics: Colloids and Nanoparticles*. Research Studies Press: Philadelphia, PA, 2003.

(2) Kayani, A. A.; Khoshmanesh, K.; Ward, S. A.; Mitchell, A.; Kalantar-zadeh, K. *Biomicrofluidics* **2012**, *6*, 031501.

(3) Khoshmanesh, K.; Nahavandi, S.; Baratchi, S.; Mitchell, A.; Kalantar-zadeh, K. *Biosens. Bioelectron.* **2011**, *26*, 1800−1814.

(4) Sonnenberg, A.; Marciniak, J. Y.; Krishnan, R.; Heller, M. J. *Electrophoresis* **2012**, *33*, 2482−2490.
(5) Nakano, A.; Camacho-Alanis, F.; Chao, T.-C.; Ros, A. *Biomicrofluidics* **2012**, *6*, 034108.
(6) Prinz, C.; Tegenfeldt, J. O.; Austin, R. H.; Cox, E. C.; Sturm, J. C. *Lab Chip* **2002**, *2*, 207−212.
(7) Moschallski, M.; Hausmann, M.; Posch, A.; Paulus, A.; Kunz, N.; Duong, T. T.; Angres, B.; Fuchsberger, K.; Steuer, H.; Stoll, D.; Werner, S.; Hagmeyer, B.; Stelzle, M. *Electrophoresis* **2010**, *31*, 2655−2663.
(8) Hashimoto, M.; Kaji, H.; Nishizawa, M. *Biosens. Bioelectron.* **2009**, *24*, 2892−2897.
(9) Vykoukal, J.; Vykoukal, D. M.; Freyberg, S.; Alt, E. U.; Gascoyne, P. R. C. *Lab Chip* **2008**, *8*, 1386−1393.
(10) Prasad, S.; Zhang, X.; Yang, M.; Ni, Y.; Parpura, V.; Ozkan, C. S.; Ozkan, M. *J. Neurosci. Methods* **2004**, *135*, 79−88.
(11) Khoshmanesh, K.; Zhang, C.; Tovar-Lopez, F. J.; Nahavandi, S.; Baratchi, S.; Mitchell, A.; Kalantar-Zadeh, K. *Microfluid. Nanofluid.* **2010**, *9*, 411−426.
(12) Tang, S.-Y.; Zhang, W.; Yi, P.; Baratchi, S.; Kalantar-zadeh, K.; Khoshmanesh, K. *Electrophoresis* **2013**, *34*, 1407−1414.
(13) Graham, D. M.; Messerli, M. A.; Pethig, R. *BioTechniques* **2012**, *52*, 39.
(14) Gielen, F.; deMello, A. J.; Edel, J. B. *Anal. Chem.* **2012**, *84*, 1849−1853.
(15) Salmanzadeh, A.; Romero, L.; Shafiee, H.; Gallo-Villanueva, R. C.; Stremler, M. A.; Cramer, S. D.; Davalos, R. V. *Lab Chip* **2012**, *12*, 182−189.
(16) Pommer, M. S.; Zhang, Y.; Keerthi, N.; Chen, D.; Thomson, J. A.; Meinhart, C. D.; Soh, H. T. *Electrophoresis* **2008**, *29*, 1213−1218.
(17) Khoshmanesh, K.; Baratchi, S.; Tovar-Lopez, F.; Nahavandi, S.; Wlodkowic, D.; Mitchell, A.; Kalantar-zadeh, K. *Microfluid. Nanofluid.* **2012**, *12*, 597−606.
(18) Hatanaka, H.; Yasukawa, T.; Mizutani, F. *Anal. Chem.* **2011**, *83*, 7207−7212.
(19) Yasukawa, T.; Hatanaka, H.; Mizutani, F. *Anal. Chem.* **2012**, *84*, 8830−8836.
(20) Khoshmanesh, K.; Akagi, J.; Nahavandi, S.; Skommer, J.; Baratchi, S.; Cooper, J. M.; Kalantar-Zadeh, K.; Williams, D. E.; Wlodkowic, D. *Anal. Chem.* **2011**, *83*, 2133−2144.
(21) Hsiung, L.-C.; Chiang, C.-L.; Wang, C.-H.; Huang, Y.-H.; Kuo, C.-T.; Cheng, J.-Y.; Lin, C.-H.; Wu, V.; Chou, H.-Y.; Jong, D.-S.; Lee, H.; Wo, A. M. *Lab Chip* **2011**, *11*, 2333−2342.
(22) Chung, C.-C.; Cheng, I. F.; Chen, H.-M.; Kan, H.-C.; Yang, W.-H.; Chang, H.-C. *Anal. Chem.* **2012**, *84*, 3347−3354.
(23) Chin, S.; Hughes, M. P.; Coley, H. M.; Labeed, F. H. *Int. J. Nanomed.* **2006**, *1*, 333−337.
(24) Khoshmanesh, K.; Akagi, J.; Nahavandi, S.; Kalantar-zadeh, K.; Baratchi, S.; Williams, D. E.; Cooper, J. M.; Wlodkowic, D. *Anal. Chem.* **2011**, *83*, 3217−3221.
(25) Franssens, V.; Boelen, E.; Anandhakumar, J.; Vanhelmont, T.; Büttner, S.; Winderickx, J. *Cell Death Differ.* **2009**, *17*, 746−753.
(26) Herker, E.; Jungwirth, H.; Lehmann, K. A.; Maldener, C.; Fröhlich, K.-U.; Wissing, S.; Büttner, S.; Fehr, M.; Sigrist, S.; Madeo, F. *J. Cell Biol.* **2004**, *164*, 501−507.
(27) Váchová, L.; Palková, Z. *J. Cell Biol.* **2005**, *169*, 711−717.
(28) Majer, O.; Bourgeois, C.; Zwolanek, F.; Lassnig, C.; Kerjaschki, D.; Mack, M.; Müller, M.; Kuchler, K. *PLoS Pathog.* **2012**, *8*, e1002811.
(29) Dementhon, K.; El-Kirat-Chatel, S.; Noël, T. *PLoS One* **2012**, *7*, e32621.
(30) Roetzer, A.; Gratz, N.; Kovarik, P.; Schüller, C. *Cell. Microbiol.* **2010**, *12*, 199−216.
(31) Hughes, M. P.; Pethig, R.; Wang, X.-B. *J. Phys. D: Appl. Phys.* **1996**, *29*, 474.
(32) Talary, M.; Burt, J.; Tame, J.; Pethig, R. *J. Phys. D: Appl. Phys.* **1996**, *29*, 2198.
(33) Alberts, B. *Essential Cell Biology*; Garland Science: New York, 2009.
(34) Salmanzadeh, A.; Kittur, H.; Sano, M. B.; Roberts, P. C.; Schmelz, E. M.; Davalos, R. V. *Biomicrofluidics* **2012**, *6*, 024104.
(35) Khoshmanesh, K.; Zhang, C.; Nahavandi, S.; Tovar-Lopez, F. J.; Baratchi, S.; Hu, Z.; Mitchell, A.; Kalantar-zadeh, K. *Electrophoresis* **2010**, *31*, 1366−1375.
(36) Khoshmanesh, K.; Zhang, C.; Nahavandi, S.; Baratchi, S.; Mitchell, A.; Kalantar-zadeh, K. *Electrophoresis* **2010**, *31*, 3380−3390.
(37) Zhou, R.; Wang, P.; Chang, H. C. *Electrophoresis* **2006**, *27*, 1376−1385.
(38) Lam, C.; James, J. T.; McCluskey, R.; Arepalli, S.; Hunter, R. L. *Crit. Rev. Toxicol.* **2006**, *36*, 189−217.
(39) Chrimes, A. F.; Khoshmanesh, K.; Stoddart, P. R.; Kayani, A. A.; Mitchell, A.; Daima, H.; Bansal, V.; Kalantar-zadeh, K. *Anal. Chem.* **2012**, *84*, 4029−4035.
(40) Wang, H. H.; Liu, C. Y.; Wu, S. B.; Liu, N. W.; Peng, C. Y.; Chan, T. H.; Hsu, C. F.; Wang, J. K.; Wang, Y. L. *Adv. Mater.* **2006**, *18*, 491−495.
(41) Rosales-Cruzaley, E.; Cota-Elizondo, P.; Sánchez, D.; Lapizco-Encinas, B. H. *Bioprocess Biosyst. Eng.* **2012**, DOI: 10.1007/s00449-012-0838-6.
(42) Kalantar-Zadeh, K.; Fry, B. *Nanotechnology Enabled Sensors*; Springer: New York, 2007.
(43) Lipke, P. N.; Ovalle, R. *J. Bacteriol.* **1998**, *180*, 3735−3740.
(44) van der Vaart, J. M.; Caro, L.; Chapman, J. W.; Klis, F. M.; Verrips, C. T. *J. Bacteriol.* **1995**, *177*, 3104−3110.
(45) Huang, Y.; Holzel, R.; Pethig, R.; Wang, X.-B. *Phys. Med. Biol.* **1992**, *37*, 1499.
(46) Gascoyne, P.; Mahidol, C.; Ruchirawat, M.; Satayavivad, J.; Watcharasit, P.; Becker, F. F. *Lab Chip* **2002**, *2*, 70−75.
(47) Cui, L.; Holmes, D.; Morgan, H. *Electrophoresis* **2001**, *22*, 3893−3901.
(48) Li, L.; Mizuhata, M.; Deki, S. *Appl. Surf. Sci.* **2005**, *239*, 292−301.
(49) Singh, G. P.; Volpe, G.; Creely, C. M.; Grötsch, H.; Geli, I. M.; Petrov, D. *J. Raman Spectrosc.* **2006**, *37*, 858−864.
(50) Xie, C.; Goodman, C.; Dinno, M.; Li, Y. Q. *Opt. Express* **2004**, *12*, 6208−6214.
(51) Sujith, A.; Itoh, T.; Abe, H.; Yoshida, K.; Kiran, M. S.; Biju, V.; Ishikawa, M. *Anal. Bioanal. Chem.* **2009**, *394*, 1803−1809.